IASS 2018 BOSTON, JULY 16-20
CREATIVITY IN STRUCTURAL DESIGN

Proceedings of the IASS Symposium 2018
Creativity in Structural Design
July 16-20, 2018, MIT, Boston, USA
Caitlin Mueller, Sigrid Adriaenssens (eds.)

Multi-physics topology optimization for 3D-printed structures

Gieljan Vantyghem*, Marijke STEEMAN[a], Veerle BOEL, Wouter DE CORTE

* Department of Structural Engineering, Ghent University
Valentin Vaerwyckweg 1, 9000 Ghent, Belgium
Gieljan.Vantyghem@UGent.be

[a] Department of Architecture and Urban Planning, Ghent University

Abstract

General topology optimization optimizes material layout within a given design space based on structural aspects. In this paper, structural topology optimization is extended to enable optimization of thermal performances. A novel multi-physics interpolation scheme is proposed and its link with 3D-printed structures is explained. Each design variable now has three optimal states: one state represents the surrounding air, having weak structural and thermal material characteristics; another state represents the solid structure with good structural, but less efficient thermal properties; a third state symbolizes a weight-efficient mesh-structure, improving the structure's thermal conductivity while retaining some structural integrity. The optimization study is performed using the GCMMA algorithm with a weighted-sum mono objective. One part of the equation aims to maximize stiffness, while the other attempts to minimize the thermal transmittance. The design domain of choice is a 2-dimensional roof component that is simply supported at the edges. Results show that using this multi-physics optimization strategy can be very useful to find the optimal trade-off between structural integrity and thermal efficiency. The maximum deflection and U-value of the optimized components are also compared to more traditional design approaches. The topologically-optimized solutions clearly outperform the others.

Keywords: Conceptual design, Topology optimization, 3D construction printing.

1. Introduction

Construction 3D printing (C3DP) refers to various technologies that use 3D printing as a core method to fabricate construction components or even entire buildings (Gardiner [1]). The potential benefits of this recent development include: faster construction, lower labor costs, reduction of waste and lower carbon emissions (Campbell et al. [2]). Additionally, the technology enables construction under harsh or dangerous environments that are not suitable for humans, (i.e. wastelands and space) (Perkins and Skitmore [3]). Most commonly, an extrusion-type nozzle is controlled automatically using large gantry robots or articulated robots with 6 or more degrees of freedom (Bos et al. [4] and Duballet et al. [5]). The material that is extruded can vary from certain types of plastic (DUS Architects [6] and WATG [7]), to clay (WASP [8]), foam (MIT [9]), or even concrete (CyBe [10], WinSun [11] and Arup [12]). A printing path is constructed by direct input from CAD, or – as being used more frequently – by advanced slicing software, which offers the additional advantage that it can easily handle complex geometries.

The ability to produce complex geometries is specific to additive manufacturing technologies. Combining this advantage with the use of large gantry robots and robotic arms, brings new possibilities to the way of production, and it introduces new design freedoms that were as yet non-existent (Gosselin et al. [13]). To cope with these changes in design freedom, advanced shape optimization tools have found their way into structural design. Topology optimization is one of such recent tools; it is a special type of optimization where the optimization process does not start from a known design (Christensen and Klarbring [14]). As such, topology optimization does not rely on an existing and typically non-optimal design. Instead, and in contrast to sizing and traditional shape optimization, it generates a

completely new design which is optimized using a mathematical formulation (Holmberg [15]). The entire design domain is first discretized by a finite element mesh, after which the contribution of every element in the mesh is determined for every new design iteration. The material lay-out is changed by adjusting the density of each element. The final topological result fully depends on the design objective and its constraints.

General topology optimization based on structural aspects only, can lead to cost minimization as well as a certain performance and efficiency maximization. The problem was first studied by Bendsøe in 1989 [16] and optimized the stiffness of a design domain for a given fraction of material. It is now well-known as the minimum compliance problem, and is also used in this study. However, considering the design of building and construction components, other aspects must be taken into consideration (Akadiri et al. [17]). These building components should be designed to meet other requirements, such as durability, sustainability, thermal and acoustical requirements. As such, a multidisciplinary approach in design optimization would be more optimal.

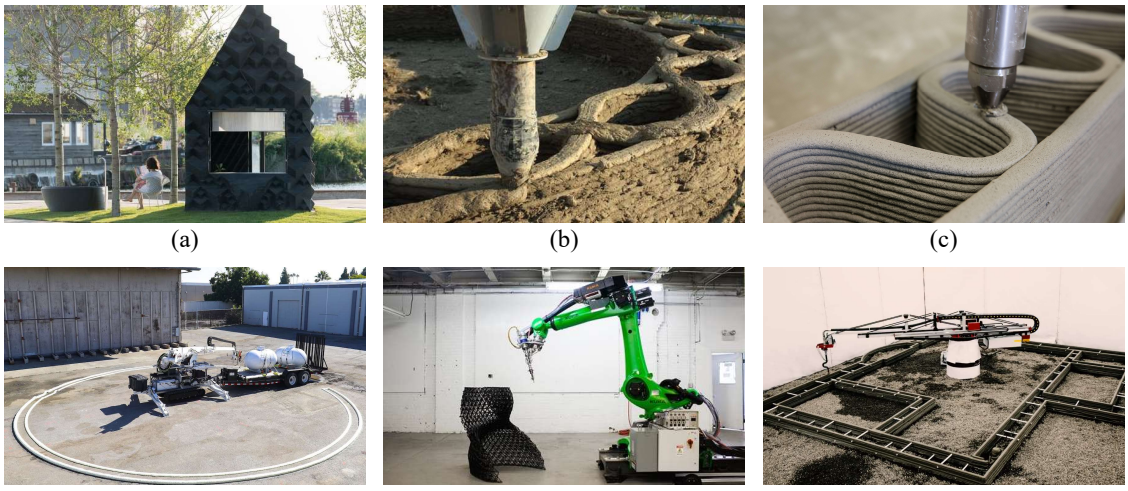

(a) (b) (c)

(d) (e) (f)

Figure 1: State-of-the-art in C3DP: A 3D-printed micro home in Amsterdam by DUS Architects (a), a low-cost 3D-printed shelter built from clay and straw by WASP (b), XtreeE's large-scale concrete 3D printer (c) a 14.6-m-diameter, 3.7-m-tall open dome foam structure by MIT (d), a 3D-printed wall structure containing a matrix of carbon-reinforced ABS plastic by WATG's Chicago-based Urban Architecture Studio (e) and Apis Cor's concrete 3D printer, printing one of America's first 3D-printed houses (f).

2. Problem formulation

In this paper, structural topology optimization is extended to cope with the thermal requirements of a building structure. As such, the heat transfer characteristics are optimized in close relation to the structure's stiffness. In the case study that is presented here, the thermal transmittance, or U-value through the design domain, and the structure's stiffness are optimized simultaneously while the maximum volume fraction is being constrained.

A 2-dimensional design domain is studied, representing a roof structure for a – to be 3D-printed – polymer-based pavilion. The roof structure is supported on its edges and is loaded by a distributed vertical load on the top and bottom surface. The boundary conditions and mechanical loadings for this problem are shown in Figure 2. Except for these distributed loadings, the case study resembles a MBB design, which is considered a benchmark problem in topology optimization. However, in contrast to other studies, the thermal performances (i.e. the U-value or thermal transmittance through the component) are also analyzed.

The units are set to the standard International System (SI-mm); lengths are given in millimeter (mm), force units are in newton (N), and the Young's modulus is given in mega-pascal (MPa), whereas the thermal load units are in watt (W), the thermodynamic temperature is given in kelvin (K), and the thermal

conductivity of a material is thus programmed in watts per millimeter-kelvin (W/mmK). In the reporting of the thermal performances, the latter are transformed into W/mK, which is the more commonly-used notation.

The dimensions of the design domain are 2400 mm x 240 mm (mesh size: 1 x 1 x 1 mm), and has a total thickness of 1000 mm. The mechanical loadings are set to 1 N/mm, derived from a 200 kg/m^2 plane load and distributed over the bottom and top surface. The difference in temperature between the inside (bottom) and the outside (top) is set to 20 K.

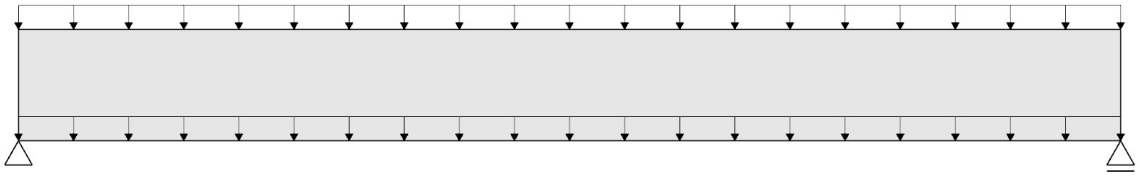

Figure 2: The design domain, boundary conditions, and external loadings for the optimization problem.

2.1. Mathematical formulation

The goal of a traditional topology optimization procedure is to find the best distribution of material which minimizes the compliance of a structure. This compliance is calculated as the integral of the strain energy density over the total volume of the design domain (Sigmund and Clausen [18]) and is often referred to as the inverse of the structure's stiffness. In the finite element analysis, a design variable is coupled to each element of the mesh. This design variable, or so-called element density (x_e), can take any value from 0 to 1. When $x_e = 0$, the element is considered as a void, while $x_e = 1$ means that an element is solid. The stiffness of an element is penalized for intermediate design variables.

Topology optimization with respect to steady-state heat transfer is very similar to that of a static mechanical problem. Similar to having a structural compliance, a thermal compliance can be calculated. Minimizing this thermal compliance will result in finding an optimal thermal conductor. Conversely, maximizing the thermal compliance will result in minimizing the thermal transmittance or U-value (Bruggi and Taliercio [19] and Vantyghem et al. [20]).

In contrast to these previous studies, the voids of the design domain (where $x_e = 0$) will simulate an outdoor environment with weak structural and thermal material properties. To comply with the minimal requirements of a building's thermal performance, a novel interpolation scheme is suggested. An additional optimal state ($x_e = 0.5$) in the material density formulation is proposed. The concept of this idea and its physical and mathematical representation is discussed in subsection 2.2.

To improve the structure's performances, the structural compliance should be minimized, while the thermal compliance should be maximized. Because the optimization algorithm works with a single objective, the thermal and structural compliance are combined into one formulation. They are converted to a weighted-sum mono-objective problem. The mathematical formulation of this problem reads as follows:

$$
\begin{aligned}
\text{Minimize}: \quad & w_1 \frac{C_{structure}}{C_{ref}} - w_2 \frac{C_{thermal}}{C_{ref}} \\
\text{s.t.}: \quad & V(\mathbf{x}) / V_{max} - 1 \leq 0 \\
\text{w.}: \quad & C_{structure} = C_s(\mathbf{x}) = \mathbf{U}^{\mathrm{T}} \mathbf{K}_s \mathbf{U} = \sum_{e=1}^{N} E_e(x_e) \mathbf{u}_e^{\mathrm{T}} \mathbf{k}_{s,e}^0 \mathbf{u}_e \\
& C_{thermal} = C_t(\mathbf{x}) = \mathbf{T}^{\mathrm{T}} \mathbf{K}_t \mathbf{T} = \sum_{e=1}^{N} \lambda_e(x_e) \boldsymbol{\theta}_e^{\mathrm{T}} \mathbf{k}_{t,e}^0 \boldsymbol{\theta}_e \\
& 0 \leq \mathbf{x} \leq 1
\end{aligned}
\tag{1}
$$

In this formulation, $C_s(\mathbf{x})$ and $C_t(\mathbf{x})$ represent the structural and thermal compliances respectively, and $V(\mathbf{x})$ the material volume that linearly depends on $\mathbf{x}$. As $C_s(\mathbf{x})$ and $C_t(\mathbf{x})$ might not have the same range of values, C_{ref} is used to normalize the values (i.e. a scaling operation is performed to make the compliances dimensionless). The next step is to select the values of w_1 and w_2 to give more importance to one of the objectives. V_{max} represents the maximum volume fraction or maximum amount of material that can be used (set to 0.5) and u_e and θ_e are the element displacement and element temperature vector. Likewise, k^0_{te} and k^0_{se} stand for the element stiffness and element conductivity matrix for an element (size: 1 x 1 x 1 mm) with Young's modulus (E_e) and thermal conductivity (λ_e). The vector of design variables is symbolized by $\mathbf{x}$, and N is the number of elements used to discretize the design domain. In total, the design domain consists of 576000 square Q4/1/1 elements.

To solve the mathematical optimization problem, the globally convergent version of MMA (GCMMA) is used. The MMA algorithm was published by K. Svanberg in 1987 [21] and is still the most widely used algorithm for topology optimization. The solver replaces the original functions by approximating functions that are based on gradient information at the current iteration point and some parameters (moving asymptotes). Different from the old MMA version, the design variables are updated using 'inner' and 'outer' iterations.

The sensitivities of the objective function C_s and C_t with respect to the element densities x_e are found using the adjoint method. Since many papers have already appeared on this topic, no further details are given about this. A review of adjoint methods for sensitivity analysis in numerical codes can be found in Allaire [22]. Finally, a density filter (Sigmund [23]) is also applied to avoid numerical instabilities like checkerboards and mesh dependencies. The original densities as well as the element sensitivities are transformed.

2.2. Material interpolation schemes

The general concept of structural topology optimization is common today, i.e. the stiffness of an element is penalized for intermediate densities. While the concept was first introduced by Bendsøe, the term 'SIMP' (as in Solid Isotropic Material with Penalization for intermediate densities) was only later coined by Rozvany et al. [24]. Most often, a power law interpolation is used; the Young's modulus is then represented by $E_e(x_e) = x_e^p$, where p symbolizes a penalization parameter (usually $p = 3$). In this paper, a similar but modified scheme is adopted, shown in Eq.(2) and proposed by Sigmund in [25], which allows the design variables to exist in the following domain: $x_e \in [0,1]$. The Young's modulus of the voids is equal to E_{min} and the Young's modulus of the solid elements is equal to E^0.

Likewise, a material interpolation scheme is created for the penalization of the element thermal conductivities (λ_e). However, a different approach is taken. This material mapping is shown in Eq.(3).

$$E_e(x_e) = E_{min} + x_e^3(E^0 - E_{min}) \tag{2}$$

$$\lambda_e(x_e) = \lambda_{min} + \left[1.75\ (0.5 - x_e)^2 + 3\ (0.5 - x_e)^3 + 3\ (0.5 - x_e)^4\right](\lambda^0 - \lambda_{min}) \tag{3}$$

$$V_e(x_e) = x_e \tag{4}$$

Very similar, λ_{min} and λ^0 contain the minimum and maximum values for the element thermal conductivity. However, in this equation, $x_e = 0.5$ contains the lowest value of λ.

The design variables clearly have three optimal states. (see also Fig. 3). One state symbolizes the surrounding air (where, $x_e = 0$), another state represents the solid structure ($x_e = 1$). Finally, a third optimal state is created ($x_e = 0.5$), which symbolizes a thermally-efficient mesh-structure made from an intermediate density.

Originally, this interpolation scheme was inspired by experimenting with different infill patterns used in desktop 3D printing. Since air may become trapped in the internal voids, certain 3-dimensional patterns (such Cubic or Tetrahedral patterns) largely increase the structure's thermal properties. The lower the block's density, the lower its thermal conductivity becomes. However, from a certain point, the voids become too large, and convection inside the voids decreases its thermal performances. Additionally, the volume fraction of the printed elements can be directly linked to its volume fraction, leading to the interpolation scheme presented in Eq.(4).

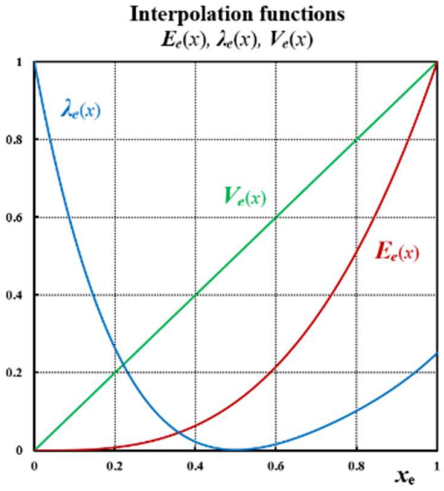

Figure 3: Mathematical formulation of the applied interpolation schemes used in this multi-physics topology optimization study: $E_e = x_e^3$, $\lambda_e = 1.75\ (0.5 - x_e)^2 + 3\ (0.5 - x_e)^3 + 3\ (0.5 - x_e)^4$, and $V_e = x_e$.

The interpolation schemes presented in Fig. 3 assume unit material properties for parameters: E^0, λ^0, and V^0. However, in this case study, the printing material is PLA. The Young's modulus of the solid material is 2400 MPa (= E^0) and its thermal conductivity is 0.265 W/mK. The Young's modulus of the voids (air) is 2.4E^{-6} MPa (= E_{min}) and its thermal conductivity is 1 W/mK (= λ^0). Following from this, the infill pattern ($x_e = 0.5$) has a Young's modulus of 300 MPa, and a thermal conductivity of 0.02 W/mK (= λ_{min}).

The principle of mapping different material properties to a range of densities, can be useful to other 3D printing technologies as well. For example, in large-scale concrete 3D printing, commonly only one extrusion nozzle is used to cast plain (or fiber-reinforced) concrete. However, when technology would allow a second nozzle to be used, a second material (e.g. a thermally-efficient substitute such as "Foamcrete" [26]) could be added to the production process. Another approach would be to actively change the rheology properties of the concrete mixture inside of the main extrusion nozzle. This idea touches the concept of a functionally-graded concrete studied by Herrmann and Sobel [27]), and could really open a whole new range of design opportunities. The topology optimization algorithms should then not only allow three optimal states but a whole range. The specific requirements of the mixture could then be determined for every location, allowing for a better assessment of the weight savings.

3. Results

The results of the topology optimization study are presented in this section. The results are spread across three groups. The first group will present the optimal distribution of material in function of only one of the sub-objectives. The first solution solves for maximum stiffness (Fig. 4a), while the second solves for maximum thermal efficiency (Fig. 4b). Finally, the second and third group will present the multi-physics optimization with the weighted-sum objective. The difference between the second and the third solution is a difference in the importance of each component in the objective.

The voids are represented in blue, the solid material in red and the intermediate (thermally-efficient) material state is displayed in green. As can be noted, the optimal solution in Fig. 4a does not include any of this green, thermally-efficient material. A very stiff frame-like structure is created. In contrast, the

solution presented in Fig. 4b only contains the thermally-efficient material; a 'green' beam is created. As mentioned before, the maximum material fraction is set to 0.5. In other words, a maximum of 50% of the 'red' material can be used. However, because the thermally-efficient material has a density of 0.5, for every element of solid material, two elements of 'green' material can be used.

(a) δ_{max} = 1.0 mm / U_{mean} = 0.89 W/mK

(b) δ_{max} = 10.6 mm / U_{mean} = 0.08 W/mK

Figure 4: First results of the topology optimization study on the design problem discussed in section 2: (a) minimum structural compliance design and (b) maximum thermal compliance design.

The beam's deflection and its U-value are also presented in the figures. Because the solution in Fig. 4a is the stiffest solution, and the beam in Fig. 4b is the most thermally-efficient solution, these values form the outer limits of the optimization problem. Increasing the thermal performance of the first solution will always decrease its stiffness, while increasing the stiffness of the second result will always decrease its thermal efficiency. The goal of the subsequent optimization studies, is to limit this performance deterioration and find the best trade-off in its material distribution.

Fig. 5a presents the first multi-material distribution. Again, the maximum volume fraction was set to 0.5. However, here, the weighted-sum objective is used. In this solution, the importance of the stiffness was set higher than that of the thermal objective. To enable comparison, the volume fraction of the 'green' and 'red' material was calculated, and two additional results were created. Fig. 5b shows a minimum compliance design for a beam with reduced height where the fraction of 'green' insulating material is put on top. Fig. 5c on the other hand, shows a design approach for which the different materials are organized in layers.

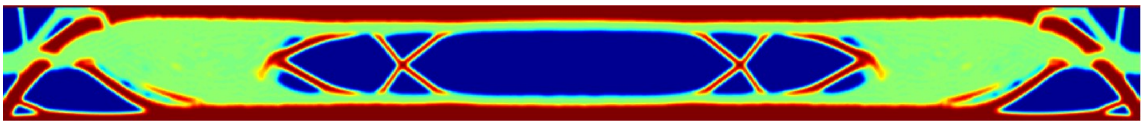

(a) δ_{max} = 1.3 mm / U_{mean} = 0.30 W/mK

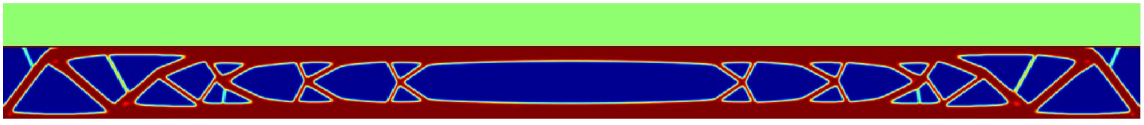

(b) δ_{max} = 2.6 mm / U_{mean} = 0.19 W/mK

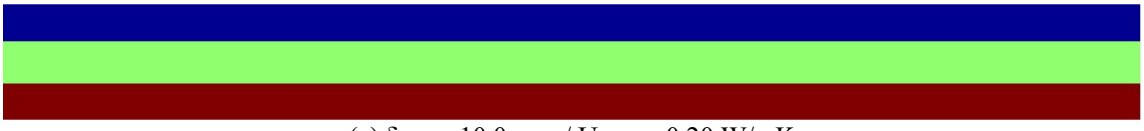

(c) δ_{max} = 10.0 mm / U_{mean} = 0.20 W/mK

Figure 5: Results of the multi-physics topology optimization study: (a) optimal design for original problem, (b) optimal structural design with insulating layer on top, and (c) layered approach for comparison.

Fig. 5a clearly presents a solution that could not have been designed by any human engineer. The result is a complex mix of the different types of material. A large portion of the beam is made by the 'green'

material, strengthened by the 'red' material in important places. The result nicely demonstrates the benefit of topology optimization; a material distribution is created that exactly finds the right trade-off in relation to the design objective. In comparison with the design from Fig. 4a, the beam has lost some of its stiffness (+30%), but its U-value has improved radically (-66%). However, the U-value of the optimized structure does not yet meet the minimal standards (0.24 W/m^{2}K for this example). In Fig. 5b and Fig. 5c, this minimal standard is met, but this comes at a large cost, as the beam's deflection has increased drastically (+160% and +900%).

An additional set of solutions is generated; now more focus is put on second term of the weight-sum objective. The weight factor (w_2) of the thermal compliance is increased. The results are presented in Fig. 6. The U-value now does meet the minimal requirement and the beam's stiffness can still be considered relatively high.

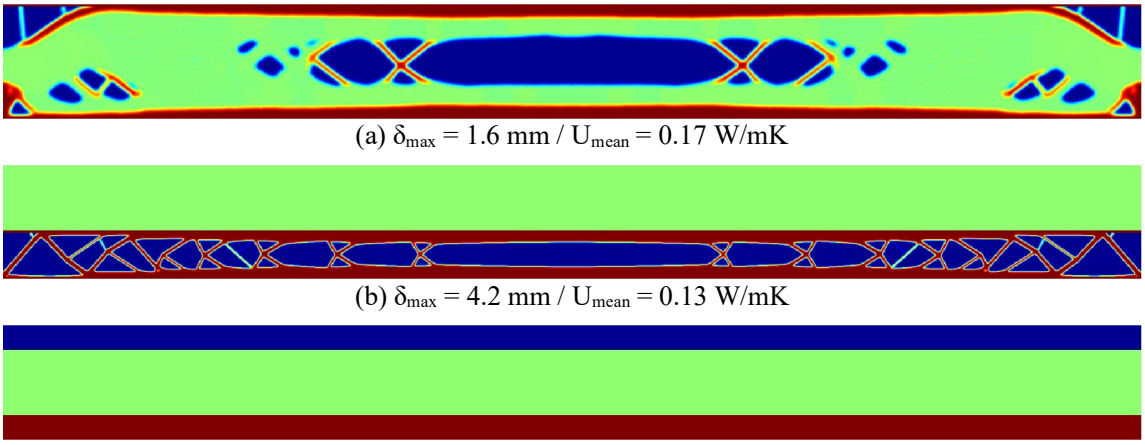

(a) δ_{max} = 1.6 mm / U_{mean} = 0.17 W/mK

(b) δ_{max} = 4.2 mm / U_{mean} = 0.13 W/mK

(c) δ_{max} = 8.3 mm / U_{mean} = 0.14 W/mK

Figure 6: Second set of results of the multi-physics topology optimization study: (a) optimal design for original problem, (b) optimal structural design with insulating layer on top, and (c) layered approach for comparison.

Again, two additional designs were generated using the same traditional approach discussed above. The topologically-optimized beam outscores the other solutions again, proving its efficiency and value. While the thermal performances increase, these gains cannot vouch for the losses in stiffness.

4. Conclusion and final remarks

3D-printing enables the production of complex geometries and offers the potential to revolutionize the building industry. However, much research is still needed to fully optimize these printing processes. Hence, while improvements are in active development, new tools for design optimization that consider the new design freedoms should be developed. In this paper, structural topology optimization was extended to cope with the thermal aspects in building design. A novel interpolation scheme was proposed to couple design densities to the element thermal conductivities. In this approach, a link was also made with the peculiarities of 3D printing such as an improvement of the thermal material properties by using 3D infill patterns.

In this paper, a roof component was optimized using a weighted-sum mono objective and demonstrated great potential for future building design. A very good trade-off between structural design and thermal efficiency could be generated. Future research on this topic could study more advanced design cases such as the one presented in Fig. 7. Here a dome structure is optimized so that the thermal transmittance through the dome is restricted to 0.24 W/m^{2}K and where the material volume is minimized. These first results sure look promising.

Acknowledgements

This research was supported by Ghent University. The authors also thank Krister Svanberg for providing the MMA optimizer code.

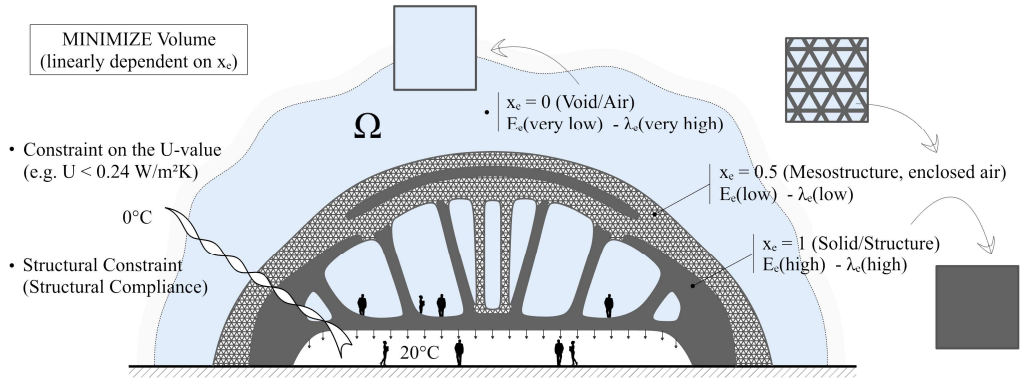

Figure 7: Multi-physics topology optimization of a dome structure where the element density variable has three optimal states. $x_e = 0$ (void), $x_e = 0.5$ (mesh-structure), and $x_e = 1$ (solid).

References

[1] J.B.Gardiner, "Exploring the Emerging Design Territory of Construction 3D Printing", Ph.D, RMIT, 2011.

[2] T. Campbell, W. Christopher, I. Olga and G. Banning, "Could 3D printing change the world." *Technologies, Potential, and Implications of Additive Manufacturing*, Atlantic Council, Washington, DC, 2011.

[3] I. Perkins and M. Skitmore, "Three-dimensional printing in the construction industry: A review", *International Journal of Construction Management*, vol. 15, no. 1, pp. 1-9, 2015.

[4] F. Bos, R. Wolfs, Z. Ahmed and T. Salet, "Additive manufacturing of concrete in construction: potentials and challenges of 3D concrete printing", *Virtual and Physical Prototyping*, vol. 11, no. 3, pp. 209-225, 2016.

[5] R. Duballet, O. Baverel and J. Dirrenberger, "Classification of building systems for concrete 3D printing", *Automation in Construction*, vol. 83, pp. 247-258, 2017.

[6] A. Frearson, "DUS Architects builds 3D-printed micro home in Amsterdam", Dezeen, 2018. [Online].

[7] E. Huen, " The World's First Freeform 3D Printed House Is Slated To Open in 2017", Forbes.com, 2018. [Online].

[8] A. Williams, "Low-cost 3D-printed shelter being built from clay and straw", Newatlas.com, 2018. [Online].

[9] K. Yurieff, "This robot can 3D print a building in 14 hours", CNNMoney, 2018. [Online].

[10] C. Clarke, "CyBe Construction 3D prints concrete drone laboratory on-site in Dubai", 3dprintingindustry.com, 2018. [Online].

[11] B. Sevenson, "Shanghai-based WinSun 3D Prints 6-Story Apartment Building and an Incredible Home", 3DPrint.com, 2018. [Online].

[12] K. Adlington, "New 3D printed house points the way to a more sustainable construction industry", Arup.com, 2018. [Online].

[13] C. Gosselin, R. Duballet, P. Roux, N. Gaudillière, J. Dirrenberger and P. Morel, "Large-scale 3D printing of ultra-high performance concrete – a new processing route for architects and builders", *Materials & Design*, vol. 100, pp. 102-109, 2016.

[14] P. Christensen and A. Klarbring, An introduction to structural optimization. [Dordrecht]: Springer, 2009.

[15] E. Holmberg, "Topology optimization considering stress, fatigue and load uncertainties", Ph.D, Linköping University, 2018.

[16] M. Bendsøe, "Optimal shape design as a material distribution problem", *Structural Optimization*, vol. 1, no. 4, pp. 193-202, 1989.

[17] P. Akadiri, E. Chinyio and P. Olomolaiye, "Design of A Sustainable Building: A Conceptual Framework for Implementing Sustainability in the Building Sector", *Buildings*, vol. 2, no. 2, pp. 126-152, 2012.

[18] O. Sigmund and P. Clausen, "Topology optimization using a mixed formulation: An alternative way to solve pressure load problems", *Computer Methods in Applied Mechanics and Engineering*, vol. 196, no. 13-16, pp. 1874-1889, 2007.

[19] M. Bruggi and A. Taliercio, "Design of masonry blocks with enhanced thermomechanical performances by topology optimization", *Construction and Building Materials*, vol. 48, pp. 424-433, 2013.

[20] G. Vantyghem, M. Steeman, W. De Corte and V. Boel, "Design of Cellular Materials and Mesostructures with Improved Structural and Thermal Performances", *Advances in Structural and Multidisciplinary Optimization*, pp. 1983-1996, 2017.

[21] K. Svanberg, "The method of moving asymptotes—a new method for structural optimization", *International Journal for Numerical Methods in Engineering*, vol. 24, no. 2, pp. 359-373, 1987.

[22] A. Grégoire, "A review of adjoint methods for sensitivity analysis, uncertainty quantification and optimization in numerical codes", *Ingénieurs de l'Automobile*, SIA, 836, pp. 33-36, 2015.

[23] O. Sigmund, "A 99 line topology optimization code written in Matlab", *Structural and Multidisciplinary Optimization*, vol. 21, no. 2, pp. 120-127, 2001.

[24] G. Rozvany, M. Zhou and T. Birker, "Generalized shape optimization without homogenization", *Structural Optimization*, vol. 4, no. 3-4, pp. 250-252, 1992.

[25] M. Bendsøe and O. Sigmund, "Material interpolation schemes in topology optimization", *Archive of Applied Mechanics*, vol. 69, no. 9-10, pp. 635-654, 1999.

[26] M. Othuman Mydin, "An Experimental Investigation on Thermal Conductivity of Lightweight Foamcrete for Thermal Insulation", *Jurnal Teknologi*, vol. 63, no. 1, 2013.

[27] M. Herrmann and W. Sobek, "Functionally graded concrete: Numerical design methods and experimental tests of mass-optimized structural components", *Structural Concrete*, vol. 18, no. 1, pp. 54-66, 2017.